

A New System of Contactless Power Transfer with Low Voltage Stress and Parasitic Capacitors Effect

Mohammad Reza Yousefi ^a, Hossein Torkaman ^{b,*}

^a Department of Electrical, Biomedical and Mechatronics Engineering, Qazvin Branch, Islamic Azad University, Qazvin, Iran

^b Faculty of Electrical Engineering, Shahid Beheshti University, A.C., Tehran, Iran

Received 2 June 2017; revised 19 August 2017; accepted 10 September 2017; available online 16 October 2017

Abstract

In this paper, a high frequency contactless power transfer (CPT) system is designed with \emptyset_2 inverter drive. This system works in 30MHz frequency and 380W power with low voltage stress and considers the inductive link parasitic capacitor effect. In the design, we formulated the inverter equations first and then suggested another design for the transmitter and the receiver coils as the energy transfer medium. Following the inverter equations, structures of proper coil are designed for a CPT system. The results of the coil and \emptyset_2 inverter designs are implemented as a bipolar circuit model which is equal to considering the inductive link parasitic capacitors. The system characteristics such as the stress, efficiency, mutual induction, field scattering, magnetic field distribution and the parameters' variations are evaluated along with analysis. The results demonstrate that the presented CPT system has high efficiency, low switching voltage stress, small passive energy storage elements and fast dynamic response.

Keywords: Contactless Power Transfer, High Frequency Inverters, ZVS, ZVDS, \emptyset_2 Inverter Class.

1. Introduction

Contactless power transfer is a young and growing technology which transfers the energy from a primary side to a secondary one needless of a wire in which the electromagnetic coupling is a method [1]. This method of wireless energy transmission is highly appropriate for places where the wire corrosion and the humidity exist. This method is also applicable in underwater. Contactless energy transmission has functional merits for static and dynamic loads like the robots and the electronic vehicles [2, 3]. This method can be regarded as an effective method for charging the transportable electronic devices such as mobiles, tablets and laptops [4-6] in which the CPT systems utilize the resonance inverters in both the primary and the secondary

sides in order to reach the maximum efficiency [7]. This issue has caused some troubles in the design and the construction of such circuits from the sight of the switching frequency and the out-put power. In other words, an inverter is limited in the mentioned areas: such as the gate supply, the output capacitor and the turn-on resistance which have significant effects on the out-put power and the efficiency. Even some troubles for PCB designing, passive components selection, measurement and evaluation analysis will also be developed.

Research in CPT systems covers an extended number of subjects such as circuit topologies, magnetic and coil designs, control and efficiency and system optimization methods. However, one serious problem that often exists in

* Corresponding author. Email: torkaman@pwut.ac.ir

most of high power CPT systems is the large passive energy storage elements due to applications in low frequencies, the voltage stress on the semi-conductor drivers and the magnetic cores. In addition, because of working in lower frequencies, the quality factor of the circuit must be selected as large which leads to increase the coils' sizes and also causes to increase the resistance and the Ohmic losses in the CPT system. A key solution to solve these problems is to increase the CPT system working frequencies from the range of KHz to MHz which leads to eliminate the ferrite core that leads to decrease the cores' magnetic losses. The resonance topologies with higher switching frequencies are often selected to decrease the switching losses. One structure that has recently earned some recognition is the E-Class inverter. The E class inverter is able to perform in higher than 1 MHz frequencies. Considering its operation in ZVS and ZVDS conditions, it is able to operate higher power in a specific voltage. It also benefits from a simpler circuit structure. The functionality of the E-Class inverter has successfully been confirmed in recent researches [8-10].

In [11-13], it is shown that in E-Class inverter, the voltage stress load decreases by putting a resonant tank in series or in parallel with the load network. By adding a resonant tank to F-class and F-1-class inverters and combining with E-class inverter, a combined inverter can be created named EF_n or E/F_n in which “n” index represents the ratio of the resonance frequency against the switching frequency which is always an integer number larger or equal to 2. If the index “n” is even, the inverter is EF_n and if odd the inverter is named as E/F_n. This added resonance network can act as a resonance tank connected in series or in parallel to the load network [12, 14-16]. As a result, the out-put power efficiency and the out-put power capacity are higher than the ones of E-class inverter in some cases and demonstrate lower voltage stresses regarding the added parallel resonance tank. The idea of combining E-Class and F-Class inverters was first presented in 2002. In this study, the frequency range, the voltage and the current wave forms were presented in assorted combinations of the resonance tank.

In [14], the design equations are presented considering the frequency as the switching frequency and the duty cycle as 50%. Also in [12], the state space model is presented for EF inverter of Figure 1. The presented model contains the ZVS and ZVDS conditions in all duty cycles and all load quality factor of the added resonance tank.

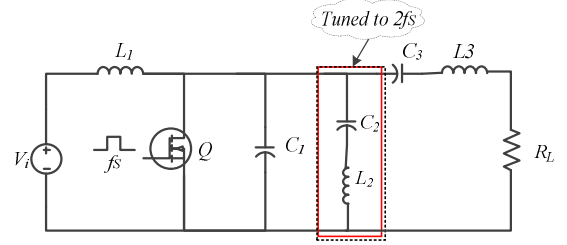


Fig. 1. The Φ_2 -Class Inverter

The presented inverter in [13] is also named as Φ_2 -Class inverter. The difference in Φ_2 -Class inverter is in utilizing the finited input inductance value or L1 instead of an infinitied inductance in EF inverter. The finite inductance of input choke is that the inductor becomes a part of the load network and makes the maximum switching frequency to increase, like E-class inverter which increases the input frequency from the factor 1 to the factor 4 with the finited input inductance [17].

The conducted analyses for Φ_2 inverters are limited to the following assumptions: duty cycle is exactly 50% and the energy capacity or Q, added from the LC resonance network are high. This issue can practically complicate the implementation of the resonant LC grid with high Q and few MHz frequency, especially for power operations. This is because the equivalent series resistance of the inductor gets large and leads to increase the losses that can make the EF and E/F usages limited compared to E-class inverters. In these inverters, the magnetic cores' utilizations must also be avoided since the saturation phenomenon leads to the loss increase. Therefore, a resonance LC network with low Q and small inductance must be regarded so as to utilize a single inductance of a multi-turn air core. Φ_2 -Class inverter increases the reflected impedance the secondary to the primary side in a CPT system, so the power flows in a lower current stress.

In this paper considering the Φ_2 -Class inerter advantages including: the elimination of the second factor harmonic, decreasing the total THD, increasing the output power capability, magnetic core elimination and increasing the reflected resistance, this inverter is utilized as the electronic drive of the presented CPT system. The structure the CPT is presented in the frequency of 30 MHz, the power 380 W and high efficiency. This paper follows the following sections:

In section II, the coil designs for the transmitter and receiver side will be presented and analyzed. In section III, a Φ_2 -Class inverter will be utilized in a CPT system

considering the resulted values in the presented design, and it will also be analyzed and classified. In section IV, considering the resulted values of the previous section, the presented system will be analyzed in the format of an equivalent circuit as a bi-polar with the parasitic capacitors of the transmitter and receiver coils. The effect of the frequency change, the distance and the loading will be investigated in this model and in the end the significant results will be concluded and presented in section V.

2. The Flat Coil Design for the CPT System

Considering the position and the location limitations in the CPT systems, the transmitter coils need to be prioritized for the designing process. Therefore, in the first step of designing a CPT system, the coil design will be developed. In the presented system the flat circular coil is utilized for the following reasons: (a) The low proximity, skin and DC losses, (b) The small value of the air gaps flux density.

Two significant and determinative factors in the CPT system coils design are the quality and the coupling coefficients which play important roles in the efficiency as well. The bigger the quality factor, the stronger the coupling (the magnetic connection) of the coils. However, one should not always expect that with increasing the quality factor, the coupling coefficient increases as well especially in the coils different sizes. On the other hand, increasing the quality factor, leads to increase the coil's size which subsequently ends up having larger Ohmic losses. The size and the geometry of the transmitter coils are significantly independent to k and Q indices. Three parameters of Ohmic resistance, inductance and the capacitance are often calculable so as to evaluate and design a high frequency flat coil which is applicable in the contactless power transfer systems. Generally, two design methods can be presented for the coils of the contactless power transfer systems. The first method is based on the coupling in which the coil is designed considering the voltages and currents of the coil and also the coupling coefficient. The second method is based on the coil geometry. In the presented system, in order to improve the coil operation in the air and accurate calculation of the parasitic capacitance around the coil, the second method is implemented.

2.1. Extraction of the Flat Coil Design Equations

As shown in Figure 2 a flat coil from the front view which is designed for the presented system in the frequency of 30 MHz in which the physical parameters are defined in Table 1. According to the presented definitions in Table 1, equation (1) can be extracted for this coil.

Table 1. The symbols characteristics utilized in the coil design

Description	Symbol	Description	Symbol
Outer diameter	D_o	DC Resistance	R_{DC}
Number of turns	N	Distance between each turns	p
Coil deep radius	c	Coil radius	a
Wire length	L	Wire diameter	w
Inner diameter of coil space	D_i	Conductivity coefficient	δ
Ohmic resistance of coils	R	Vacuum permeability	μ_0
Receiver radius	R_j	Frequency	f
Transmitter radius	R_i	Mutual Inductance	M
Coupling coefficient	k	Distance between coils	d

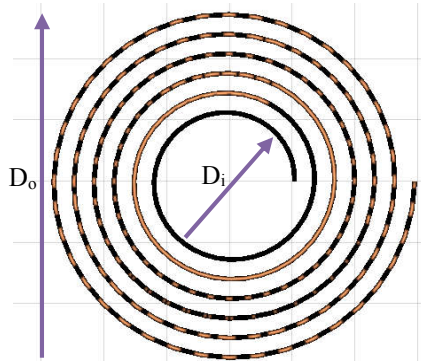


Fig. 2. The designed flat coil in the frequency of 30 MHz

$$D_i = D_o - 2N(w + p) \quad (1)$$

$$a = \frac{1}{4}(D_o + D_i)$$

$$L = \frac{1}{2} N \cdot \pi (D_o + D_i)$$

$$c = \frac{1}{2}(D_o - D_i)$$

According to the aforementioned equations, the values of the length, the outer diameter, the coil radius and the internal coil radius can be calculated for a more accurate evaluation of the flat coil.

2.1.1. The Inductance Calculation

One of the most important values for evaluating the accurate functionality of a CPT system is the precise calculation of the inductance value of the transmitter and receiver coil.

$$L(H) = \frac{N^2(D_o - (w + p)^2)}{16D_o + 28N(w + p)} \times \frac{39.37}{10^6} \quad (2)$$

In this equation, the values are in meters and the inductance is calculated in Henry. The above equation is not appropriate for the coils with low turning ratio or the coils in which the coil pitch is too larger than the wire diameter or if the ratio $\frac{c}{a} > 0.2$ exists.

2.1.2. Calculating the Capacitance Around the Flat Coil

Since the formed parasitic capacitance in the proximity of a flat coil that is utilized in CPT systems in high frequencies has a significant numerical value, calculating this value has a great importance so as to determine the external capacitance added for the resonance.

The formed capacitance in the coil proximity is a function of the conductor conductivity coefficient, the diameter of each turn of the coil, the total number of the turns and the coil pitch. By increasing the number of the turns, the value of the formed capacitance in the coil proximity increases significantly and non-linearly. The value of the proximity capacitance is often within PF scale and calculable from equation (3).

$$C(F) = \frac{1}{(2\pi f)^2 L} \quad (3)$$

In some applications the value of the coil proximity capacitance can be used instead of the added capacitance in the resonance tank.

2.1.3. Resistance

There are losses in two regions of a flat coil: the conduction losses and the losses of radiation losses. Since the wavelength is often much longer compared to the coil (almost 22 meters at 13 MHz frequency), the radiation losses are disregarded. The conduction loss is a function of the skin effect and the proximity, however, in the flat coil used in the presented CPT system, the factor that makes changes to the

coil resistance value is the coil pitch “p”. This has a reverse relationship with the Ohmic value of the resistance because of the proximity effect and this effect is non-linear. The Ohmic value of the resistance can be calculated from the Kaiser's high frequency model.

$$R = R_{dc} \frac{w}{4\delta} = \sqrt{\frac{4\pi\mu_0}{\sigma}} \frac{N(D_o - N(w + p))}{w} \quad (4)$$

$$R_{dc}(\Omega) = \frac{1}{\sigma\pi(\frac{w}{2})^2} \quad (5)$$

$$\delta = \frac{1}{\sqrt{\pi\sigma\mu_0 f}} \quad (6)$$

In which σ the Copper's conductivity coefficient and equals $59.6 * 10^6$.

2.1.4. The Quality Factor

Since the series resonance is utilized in the presented system, the quality factor can be defined as the equation (7).

$$Q = \frac{1}{R} \sqrt{\frac{L}{C}} \quad (7)$$

Using the extracted equations (2)-(6) defined in the previous sections and replacing them in equation (7), the quality factor of the flat coil is defined as the equation (8).

$$Q = \frac{39.37}{10^6} \sqrt{\frac{f\pi\sigma}{\mu_0}} \cdot \frac{wN(D_o - N(w + p))}{8D_o + 14N(w + p)} \quad (8)$$

From which designing a coil with a high value of Q is possible and ensure resonance at the desired operating frequency.

2.1.5. Coupling Coefficient and the Mutual Inductance

The amount of the generated flux by the transmitter which passes through the receiver determines the coupling coefficient. In CPT systems, the coupling coefficient is used instead of the mutual induction for the simplicity. The coupling coefficient is a function of the geometric shape of the coil, the distance between coil, and the coils' direction toward one another. Assuming the coil angles as zero, the mutual inductance of the transmitter and the receiver coils can be calculated from the equation (9).

$$M = \sum_{I=1}^{N_{TX}} \sum_{J=1}^{N_{RX}} \mu_0 R_i R_j \int_0^{\pi} \frac{\cos \theta d\theta}{\sqrt{R_i^2 + R_j^2 + d^2 - 2R_i R_j \cos \theta}} \quad (9)$$

In which the coupling coefficient is defined as follows [18-21].

$$K = \frac{M}{\sqrt{L_i L_j}} \quad (10)$$

2.2. Review of the Flat Coil Design in the Presented System

According to the previous sections, the design process of the flat coil can be explained as follows. Firstly, the maximum allowed size should be determined since the size of the receiver coil is of importance regarding the considered application. Then a size range must be defined for the transmitter coil. In the following, the maximum Q must be determined for the transmitter and the receiver and finally, an appropriate geometry (one of the different kinds of the flat coils like square, polygon and circular) must be regarded for the transmitter and the receiver in order to reach the best possible efficiency in the coil design. The design result of this section is as follows:

- According to equation (9), one can come to conclude that the maximum coupling coefficient is reached for two same size coils; as a result, two same size coils are implemented so as to reach the maximum coupling coefficient in the presented system.

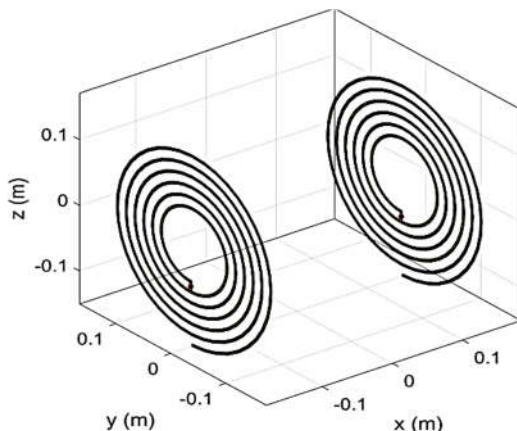


Fig. 3. The designed flat coils for the frequency of 30 MHz

- As stated in the previous section, the resistance value of the skin effect increases non-linearly. So for creating a small resistance, large values for Q must be utilized. Therefore, it is better for the designed coils to not get too compact. On the other hand, selecting a large value of the quality factor leads to increase the inductance and subsequently increases the length of the conductor and hence the Ohmic resistance. In the presented system, the large value of the quality factor is compensated by applying the frequency of 30 MHz, so the quality factor is selected as 12 so that either the skin effect is decreased and the desired quality factor gets resulted.
- When designing a flat coil, the calculation resonance frequency is of great significance. One appropriate solution to find the resonance frequency is the study of the coil impedance. The impedance variations that includes the resistance and the reactance changes, versus the frequency variations is illustrated in the Figure 4. Since this flat coil is a magnetic resonance, it is witnessed that a Lorentz shape reactance in the frequency band of 28 to 31 MHz is resulted which has already been expected. The reactance variation range is variable until 1000 Ohm, compatible to the resulted resonance frequency.

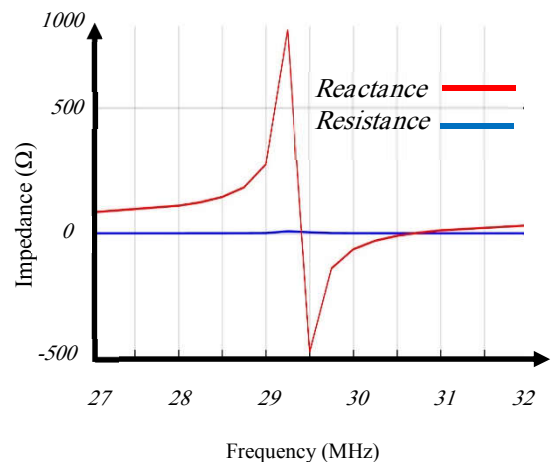


Fig. 4. The Frequency-impedance variations

- According to the calculations in section III, the inductance value of the primary coil is derived as 7.4 μH. According to this value, a flat circular coil (the flat circular coils have better flux density compared to the other types) is considered for the presented system which has the dimensions of outer diameter

D0=15 cm, inner diameter Di=5 cm, number of turns 6.5 and the conductor diameter of 18 AWG.

3. Design and Modelling of the CPT Transmitter and Receiver Circuits

The current, in the primary coil of an inductive link has to be alternating in order to generate an alternating magnetic field to induce a voltage in the secondary coil. In this regard, a DC to AC inverter is needed. In order to present higher efficiencies, the inductive links need large amounts of energy because of the possibility of the changing distances. Only specific classes of switching inverters can fulfil such conditions. As expressed in section I, a \emptyset_2 -Class Inverter can operate in high frequencies. Considering the second harmonic elimination in this inverter, it demonstrates a low voltage stress which has made it to operate in high levels of voltage and power. Considering the merits of this inverter, \emptyset_2 -Class Inverter is used as a driver of the transmitter circuit.

3.1. The Design of \emptyset_2 -Class Inverter in the Presented CPT System

According to Figure 1, the circuit diagram of \emptyset_2 -Class Inverter, L_2 and C_2 are the inductance and the capacitor of the resonance tank respectively which are added to decrease the switching voltage stress. They are adjusted in twice the switching frequency. The output network inductor L_3 and the capacitor C_3 are adjusted. They are adjustable with the switching frequency so as to create ZVS and ZVDS conditions. C_1 is the switch parallel capacitor, L_1 is the finite input inductance. \emptyset_2 -Class Inverter is the improved form of E-class inverter. So the existing equations of designing E-class inverters can also be utilized to design \emptyset_2 -Class inverter. Note that the equations 11-13 which are mentioned in [22] are used to calculate L_1 , L_2 and C_2 . Since the second harmonic is the largest harmonic of the system, these values are designed in twice the value of the switching frequency so as to eliminate this harmonic and decrease the switch voltage stress.

$$L_1 = \frac{1}{9\pi^2 f^2 C_f} \quad (11)$$

$$L_2 = \frac{1}{15\pi^2 f^2 C_f} \quad (12)$$

$$C_2 = \frac{15}{16} C_f \quad (13)$$

In specific applications, \emptyset_2 -Class Inverter can be designed and utilized in “n” times the switching frequency in order to eliminate the third harmonic or higher [23]. As it is depicted in Figure 5, according to the developed designs for \emptyset_2 -Class Inverters, the switch voltage stress values of \emptyset_2 -Class inverter compared to E-class inverter have decreased for as much as 1 KΩ and 200V respectively in the same amounts of the load.

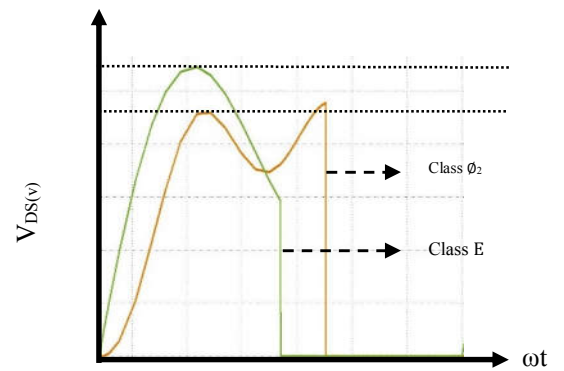


Fig. 5. The switching voltage stress of E-class inverter compared to \emptyset_2 -class inverter

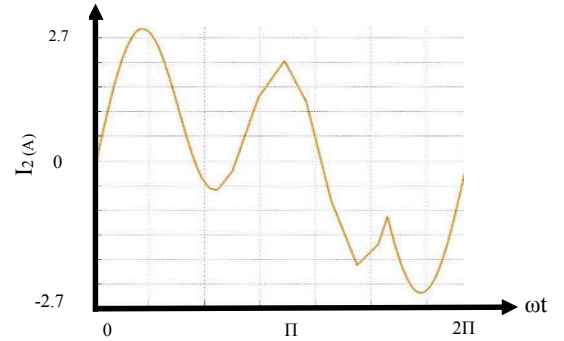


Fig. 6. The current I_{LMR} of \emptyset_2 -class inverter

As it is observed in Figure 5, the stress voltage of \emptyset_2 switch inverter is almost 460V which has decreased as 17% compared to E-class inverter because of eliminating the second harmonic by the resonant tank which is parallel to the switch. This voltage decrease is equal to 90V. In the presented application, the decrease of the switch stress voltage leads to increase the output power capacity of \emptyset_2 -Class inverter from 0.09 to 0.13 compared to E-class inverter. Regarding the capacity change, the duty cycle also has changed from 50% to 37%. Figure 6 illustrates and compares the duty cycles of \emptyset_2 -Class and E-class inverters in the same load values.

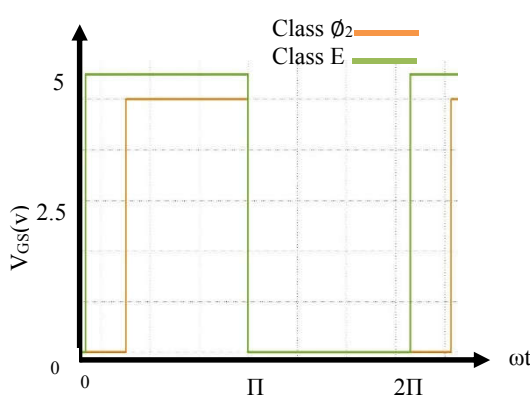


Fig. 7. The applied gate voltages of E-class and \emptyset_2 -Class inverters in 50% and 37% duty cycles

Employing \emptyset_2 -Class inverter in CPT system has the following advantages:

- Because of the low voltage stresses, inexpensive switches can be employed for the similar applications compared to E-class inverters. In high powers, this cost difference is more touchable and the semiconductors benefit from longer mechanical age.
- The output power capacity, the maximum operation frequency and the efficiency of this inverter are higher compared to the similar topologies, E-Class and D-Class inverters. Also, compared to these two classes, this inverter has higher input voltage which leads to ripple and input dc current decrease which subsequently the non-capacitive parasite effect of Mosfet decreases.
- The optimum duty cycle in this class of inverter can be between 37% and 40% while in the similar system of E-class has the optimum value of 50%.
- Because of operating in high frequencies and small quality factor of this system, air-core inductors are employed. Therefore, because of eliminating magnetic losses of the core, this inverter has higher efficiency compared to D-Class and E-Class inverters.

3.2. The system of the Presented CPT with \emptyset_2 -Class Drive

In the presented CPT system of Figure 8, \emptyset_2 -Class inverter is employed which has been designed in section 3.1 as the driver of the transmitter circuit. The L3 value of inductance is going to be employed in two roles as the

primary coil and the resonance inductor. As it was expressed in section 2.2, for flat coils, the maximum coupling coefficient happens for two same size coils, therefore, in the presented structure, the receiver coil is selected in same inductance value and geometry similar to the ones of L3. The capacitor Cs is designed and calculated, parallel to the secondary coil, considering the load value.

Creating the resonance condition by capacitor Cs, the reactance of the secondary circuit can be eliminated through which some features will be followed:

- Causes the reflected impedance to increase, i.e. the distance between the transmitter and the receiver gets decreased
- The impedance of the secondary coil gets decreased and subsequently, the power loss decreases.
- The circuit capability of power transmission increases compared to the non-resonant mode.

The presented system of Figure 8 features the input voltage of 200V in 30 MHz frequency with the ability of providing output power of 380V to the load.

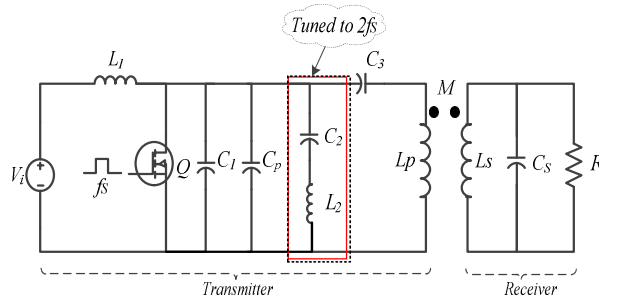


Fig. 8. The presented CPT system

The frequency range of the designed inverter in section 3.1 is measured and illustrated in Figure 9 in which the resulted THD is equal to 3.95%. By re-measuring the THD value, this time in the receiver circuit of the CPT system presented in Figure 8, it is observed that the value of THD changes to 14.2% by changing the distance of the transmitter and the receiver to 5 cm.

As it is observed in Figure 9, the second harmonic is eliminated which is the largest harmonic of the presented CPT. This elimination has led to decrease the voltage stress in an equal transmission distance compared to E-class inverter.

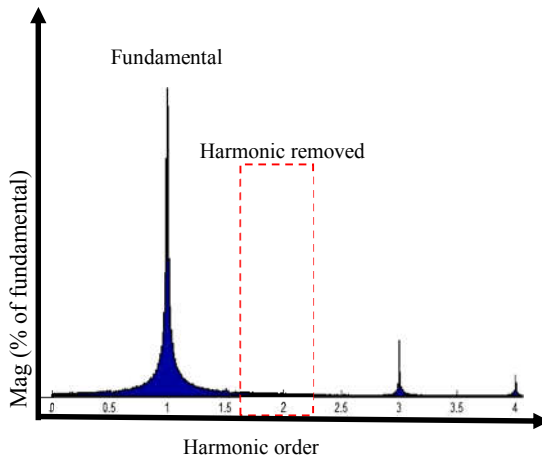


Fig. 9. The frequency range according to the harmonic hierarchy in the presented system

4. The Equivalent Circuit of the Presented System and the Parasitic Capacitance

In order to analyze the operation of the presented system of Figure 8 in various frequency and coupling coefficient values and also investigate the loading effect on the circuit operation and the reflected impedance, the equivalent circuit of the inductive link can be extracted, considering the resulted numerical design values of Table 2. This equivalent circuit of the inductive link includes the transmitter and receiver of the presented model along with the parasitic capacitance. Figure 10 shows the resulted equivalent circuit. The capacitors C_T and C_R contain the transmitter and receiver resonance capacitors, respectively. C_{ST} and C_{SR} represent the parasitic capacitance of the transmitter and receiver circuits in the inductive link region and the total equivalent capacitance is equal to $C_{RE}=C_{SR}+C_R$.

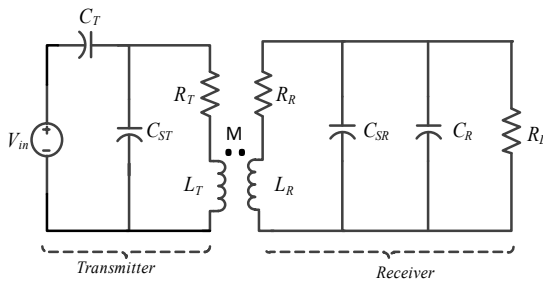


Fig. 10. The SP model of the CPT system along with parasitic capacitance

In order to evaluate the presented model, the efficiency needs to be calculated in the transmitter and receiver circuits. In this regard, by applying KVL in the transmitter and the receiver circuit, the equation (14) and (15) are resulted.

$$V_{in} - \frac{I_T}{j\omega C_T} - I_{LT}(R_T + j\omega L_T) + j\omega M I_R = 0 \quad (14)$$

$$\frac{I_T - I_{LT}}{j\omega C_{ST}} - I_{LT}(R_T + j\omega L_T) + j\omega M I_R = 0 \quad (15)$$

Similarly, by applying KVL in the receiver circuit and after simplifications and insertion of $C_{SR}+C_R=C_{RE}$, the equation (16) will be resulted.

$$j\omega M I_{LT} - I_R \left[j\omega L_R + R_r + \frac{R_L}{1 + j\omega C_{RE} R_L} \right] = 0 \quad (16)$$

After simplification of the receiver circuit impedance, it can be divided into two real and imaginary parts.

$$R_{rec} = \frac{R_r + R_L + \omega^2 R_r C_{RE}^2 R_L^2}{1 + \omega^2 C_{RE}^2 R_L^2} \quad (17)$$

$$X_{rec} = \frac{\omega L_R - \omega C_{RE} R_L^2 + \omega^3 L_R C_{RE}^2 R_L^2}{1 + \omega^2 C_{RE}^2 R_L^2} \quad (18)$$

So the impedance of the transmitter circuit can be obtained from equation (19).

$$Z_{tran} = \frac{1}{j\omega C_T} + \frac{(R_r + R_{ref}) + j\omega L_R}{1 + (R_r + R_{ref}) j\omega C_{ST} - \omega^2 L_R C_{ST}} \quad (19)$$

By replacing the equation (16) in equation (14), the reflected impedance can be obtained from equation (20).

$$Z_{ref} = \frac{\omega^2 M^2 (\omega^2 R_r C_{RE}^2 R_L^2 + R_r + R_L)}{(-\omega^2 L_r C_{RE} R_L + R_r + R_L)^2 + (\omega L_r + \omega R_r C_{RE} R_L)^2} + \\ j \left[\frac{\omega^2 M^2 (\omega C_{RE} R_L^2 - \omega^3 L_R C_{RE}^2 R_L^2 - \omega L_R)}{(-\omega^2 L_r C_{RE} R_L + R_r + R_L)^2 + (\omega L_r + \omega R_r C_{RE} R_L)^2} \right] \quad (20)$$

For further simplifications the real and imaginary parts of the reflected impedance can be separated.

$$R_{ref} = \frac{\omega^2 M^2 (\omega^2 R_r C_{RE}^2 R_L^2 + R_r + R_L)}{(-\omega^2 L_r C_{RE} R_L + R_r + R_L)^2 + (\omega L_r + \omega R_r C_{RE} R_L)^2} \quad (21)$$

$$X_{ref} = \frac{\omega^2 M^2 (\omega C_{RE} R_L^2 - \omega^3 L_R C_{RE}^2 R_L^2 - \omega L_R)}{(-\omega^2 L_r C_{RE} R_L + R_r + R_L)^2 + (\omega L_r + \omega R_r C_{RE} R_L)^2} \quad (22)$$

Since the imaginary part of the reflected impedance is equal to zero because of the resonance, $X_{ref}=0$, the real part of the reflected impedance should be regarded in the final equivalent circuit. The final equivalent circuit is extracted as Figure 11.

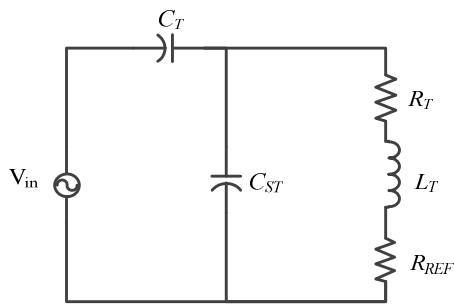


Fig. 11. The equivalent circuit of the CPT system along with the parasitic capacitance and reflected impedance.

The imaginary part of the equivalent circuit is eliminated because of the resonance. Therefore, the values of C_T and C_R is resulted by resetting the imaginary part to zero.

$$C_T = \frac{2\omega_0^2 L_T C_{ST} - \omega_0^2 C_{ST}^2 (R_T + R_{ref})^2 - \omega_0^4 L_T^2 C_{ST}^2 - 1}{\omega_0^2 C_{ST}^2 (R_T + R_{ref})^2 + \omega_0^4 L_T^2 C_{ST} - \omega_0^2 L_T} \quad (23)$$

$$C_R = \frac{R_L \pm \sqrt{R_L^2 - 4\omega_0^2 L_R}}{2\omega_0^2 L_R R_L} \quad (24)$$

The efficiency of the transmitter and the receiver is calculated as below:

$$\eta_T (\%) = \frac{R_{rec}}{R_T + R_{rec}} \times 100 \% \quad (25)$$

$$\eta_R (\%) = \frac{R_L}{R_r + R_L + \omega_0^2 R_R C_{RE}^2 R_L} \times 100 \% \quad (26)$$

The total efficiency is resulted from multiplying the transmitter efficiency by the receiver one. As a result, since the transmitter efficiency is equal to the proportion of the receiver's given power to the transmitter's one, and the receiver's efficiency is equal to the proportion of the load's given power to the total power of the receiver, the total efficiency of the entire system is resulted from the equation (27).

$$\begin{aligned} \eta (\%) &= \frac{M^2 R_L}{R_T [\gamma] + M^2 [\zeta]} \times 100 \% \quad (27) \\ \gamma &= \frac{L_R (L_R + R_r + R_r C_{RE} R_L)^2}{(C_{RE} R_L^2 - L_R)} + (L_R + R_r C_{RE} R_L)^2 \\ \zeta &= \frac{(R_r + R_L) L_R + (C_{RE} R_L^2 - L_R) R_r}{L_R} \end{aligned}$$

4.1. The Results and Analysis of the Presented Model

According to the fabricated model in the previous section, the results of this modelling is in the following subsections:

4.1.1. The Effect of the Frequency on the Power and the Output Efficiency

According to equation (27), the efficiency of the presented system is calculated in various operating frequencies. The results are illustrated in Figure 12. In this figure, the resonance capacitor which is suitable for the coils is calculated with regarding the parasitic capacitance of the inductive link in each stage in the distance of 5 centimetres. It is observed that within the range of 30 MHz frequency, the efficiency is fixed and equal to 95%. So this frequency can be regarded as appropriate operating frequency for this application which makes the passive elements of the system to shrink.

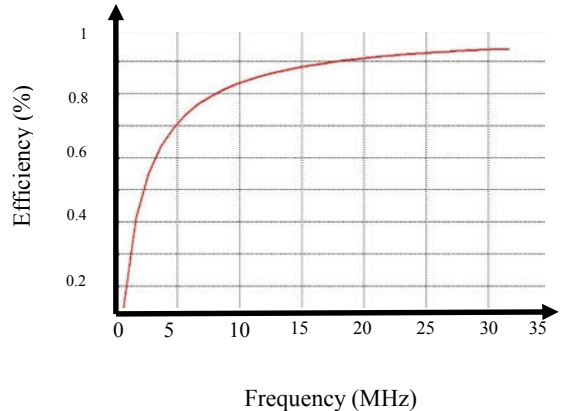


Fig. 12. The efficiency versus the operating frequency

Also by obtaining the value of I_R from the equation (16) and calculating the load voltage, the given power to the load can be calculated from the equations 28 and 29 by applying KVL in the receiver circuit.

$$V_L = I_R \left[\frac{R_L}{2 + j\omega C_{RE} + R_L} \right] \quad (28)$$

$$P_L = \frac{V_L^2}{R_L} \quad (29)$$

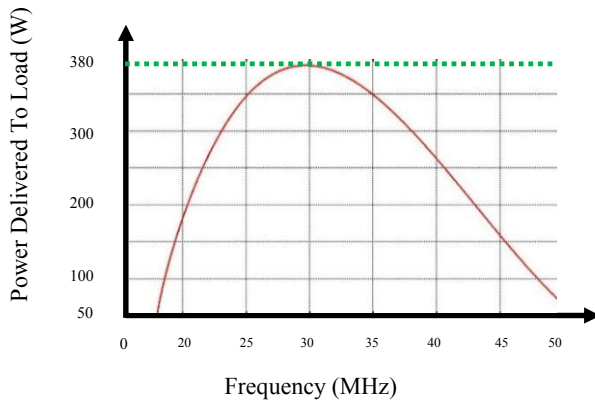


Fig. 13. The frequency variations versus the given power to the load

According to diagram 13 it is observed that the given power to the load increases as the frequency increases until 30 MHz which is the desired operating frequency. Then, as the frequency increases, the given power to the load decreases. As it is observed, the maximum power of 380W is reached for the presented system in the frequency of 30 MHz.

4.1.2. The Loading Effect and Distance Change on the Reflected Resistance

Figure 14 shows the load change effect and the frequency on the reflected resistance in various resonance frequencies. It is observed that constantly, $X_{ref}=0$ and $Z_{ref}=R_{ref}$ because of the resonance. The resistance seen from the primary side in the frequency of 30 MHz and in the load of 1.5 KΩ has the value of 20Ω which shows the appropriate operating point and the maximum reflected resistance.

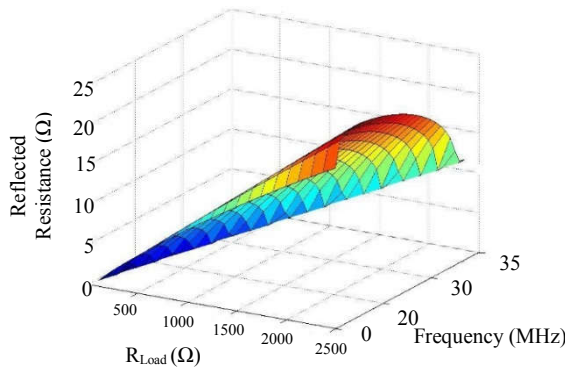


Fig. 14. The frequency and load influences on the reflected resistance

The larger the primary side of the circuit sees the resistance of the secondary side, the larger efficiency is transferred. According to diagram 14, it can be interpreted that the high frequencies are appropriate for large loads. In

the presented model, since a parallel capacitor is used in the receiver circuit for the resonance creation, it is observed that by shortening the distance, the observed resistance by the primary side increases. One of the problems that leads to huge energy loss in long distances is the equivalent resistances of the transmitter and the receiver coils and the passive elements of the circuit which make the CPT systems limited.

Table. 2. The Values Of ϕ_2 -Class Parameters and Inductive Link at 30 MHZ

Parameters	With considering E-class inverter	With considering maximum switching frequency
L_1	625.4 nH	35.3 μ H
L_2	375.26nH	1.18 μ H
C_2	18.75 pf	5.95 pf
C_1	16.04 pf	18.6 pf
C_p	20 pf	9.33 pf
C_3	4 pf	4.87 pf
L_p	7.4 μ H	6.95 μ H
L_s	7.4 μ H	6.95 μ H
C_s	13.5pf	4.69 nf
R_L	100-1kΩ	100-1kΩ
V_{in}	200 v	200-329 v
P_o	380	380
Duty cycle	37.5%	37.5%
M	2.33-3.86 μ H	2.33-3.86 μ H
Distance	0-5 cm	0-5 cm

One recommended method that is applicable for longer distances is the utilization of the parallel capacitor in the secondary side, because it leads to a decreased current and subsequently a decreased power loss in ESR (Equivalent Series Resistance) resistances. Therefore, it can be stated that if the load value is very smaller than the secondary reactance, it is better to use series capacitor in the receiver circuit. If the load value is significantly larger than the secondary reactance it is better to use the parallel resonance.

Figure 15 shows the distance effect from 1 to 10 cm and the loading effect on the reflected resistance. It will be observed that in the load value of 1.5 KΩ the reflected resistance value is equal to 18Ω. So the appropriate load value for this application can be selected as 1.5 KΩ. By increasing the distance from 1 to 10 cm and decreasing the load from the amount of 1.5 KΩ, the observed resistance from the primary circuit has got less than 18Ω which decreases to 2 Ω in the distance of 10 cm from the reflected resistance.

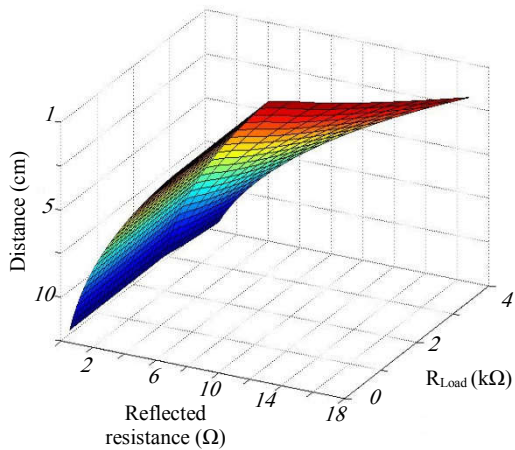


Fig. 15. The influence of the Distance and the load value on the reflected resistance

4.1.3. The Effect of Distance and Frequency Change on the Magnetic Connection of the Coils

According to Figure 10, since the resulted equivalent circuit can also be modeled as a bi-polar (one port represents the input that is fed by the source and the other side represents the output which feeding the load), the power transmission scattering can be calculated by measuring the linear magnitude scattering parameters ($|S_{21}|$). This is an important parameter for analysis a vector network at high frequencies. S_{21} is defined as follows:

$$S_{21} = 2 \frac{V_{load}}{V_{source}} \left(\frac{R_{source}}{R_{load}} \right)^{\frac{1}{2}} \quad (30)$$

The difference of using equation (30) and other similar parameters like Y parameters, Z parameters, H parameters, T parameters and ABCD parameters is that the above parameter employs the matched loads instead of using the open circuit and short circuit conditions for specifying the circuit features. This type of description in high frequencies is way simpler than the open circuit and short circuit conditions.

Figures 16 and 17 illustrate the S_{21} value change in the frequency of 30 MHz. It is observed that the coupling between the two coils, increases from 0.2 to 0.8 linearly by the distance reduction from 0.4 to 0.2 in the frequency of 30 MHz. this trend is approximately equal to $1/d^3$ (d : the distance between the two coils). Therefore the system

efficiency increases through the distance reduction to an extent in which it reaches the critical point when S_{21} is equal to 0.95. When the magnetic coupling of two coils exceeds the value of 0.95, the system remains in its peak of efficiency. In this point, the frequency separation is obvious in the distance of 0.2 cm. In the frequency splitting part, the coupling of the two coils gets weaker until when the two separated parts get convergent again in the frequency of $f=30$ MHz. This point can also be named as the critical coupling point which represents the longest distance in which the maximum efficiency is still available. Figure 16 actually shows a parametric study of the system “S” as a function of the transfer distance.

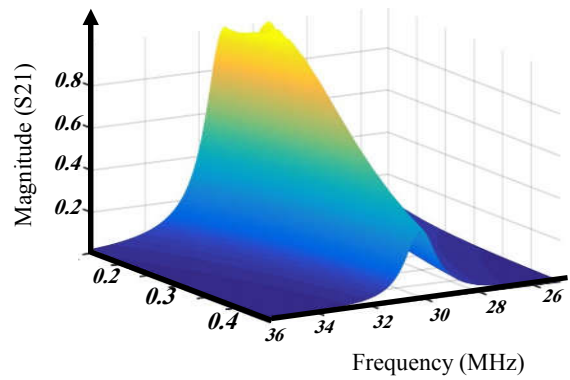


Fig. 16. The S_{21} as a function of the frequency and the distance

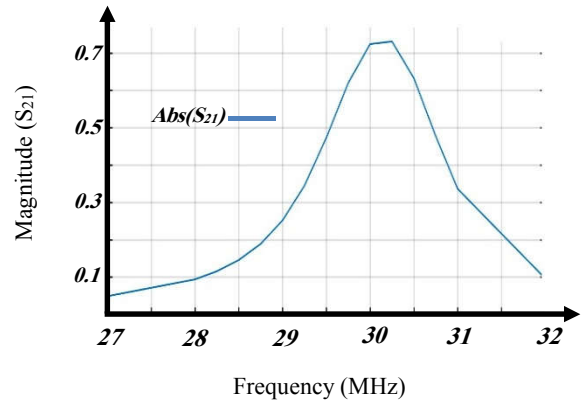


Fig. 17. S_{21} variations versus the frequency

The results of the models’ simulation shows that in frequencies less or higher than 30 MHz the coupling value between the two coils gets decreased. Figure 17 has also shown the S value analysis. As it is observed, the system efficiency changes rapidly by the frequency and coupling variations between the transmitter and the receiver. The peak efficiency is in the frequency of 30 MHz when the system is

in the resonance mode and the two coils have a strong magnetic coupling (S_{21}) of 0.7. The fields around a high frequency transmitter are called the near-field which are far or near to the emitting source in which the standard of the remoteness and the nearness is the wavelength of the emitted waves. According to the S_{21} parameter, since a flat designed coil is a magnetic resonator, the dominant field component of this coil is the magnetic field. If the near-field effect is plotted, a strong local field in the distances of 0 to 15 cm will be observed in this circular flat coil.

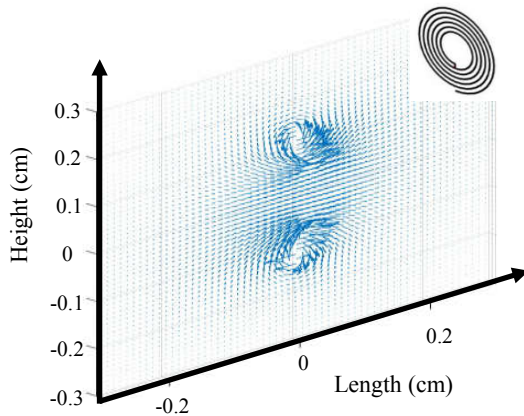


Fig. 18. The magnetic field distribution in the flat designed coil

The following considerations are taken into account of the design procedure:

- In order to design and analyze the presented system, the frequency of 30 MHz is utilized since this frequency is desirable for designing small volume CPT systems. Also it is a definite and desirable frequency for analyzing the broadband and drawing the points in the space for near-field systems.
- It was shown that if there is no limitations for the coil designs, the maximum efficiency happens for the two same size coils. Therefore, in the presented system, the two same size coils are employed in the circuits of the transmitter and the receiver. However, if there are coil design limitations, according to equation 31 an appropriate coil can be designed.

$$\frac{V_2}{V_1} \propto K \sqrt{\frac{L_2}{L_1}} \quad (31)$$

- One of the most important parameters for high frequency inductors is the value of their stray capacitor, since the presented system has been

designed based on the electromagnetic coupling. If the value of these stray capacitors is not calculated, an undesired resonance in the transferred efficiency may be resulted. Therefore, the effect of the formed capacitors around the inductive link is calculated and employed in the design and analysis.

- A \emptyset_2 -Class inverter whose parameters are extracted based on the E-class inverter design equations is designed in the frequency of 30 MHz in which the THD is suitable and equal to 3.85%. In the following, this designed inverter is utilized in a CPT system with the frequency of 30 MHz and the model of its inductive link is analyzed and investigated. It is shown that the presented system demonstrates the efficiency of 95%.
- According to the frequency range of the presented system, it can be concluded that \emptyset_2 -Class inverter does not present the second harmonic, thus demonstrates lower THD against an E-Class inverter. In the following, according to the results, the switch voltage stresses will be lower and. \emptyset_2 -Class inverters will also have better adjustability EMI compared to E-class inverters.

5. Conclusion

This paper deals with the investigation and the design of a CPT system which works upon a \emptyset_2 -class inverter. An analysis has been presented based on the coil design in the contactless system. According to this design, a coil with the appropriate dimensions and geometry for a CPT system can be presented. The optimum values for the \emptyset_2 -class inverter were extracted from the numerical design of an E-class inverter. The constructed inverter in the CPT structure was operated and it was shown that the voltage stress has decreased to 17% compared to E-class inverter. Therefore, the presented system has a higher power output capacity. In the following, a bipolar equivalent circuit was presented for the presented structure in which the CPT system was analyzed magnetically and from the point of the frequency. The analysis of the presented circuit has shown that in the frequency of 30 MHz the efficiency is 95% with the THD index is 3.85% along with the maximum efficiency, power and coupling.

References

- [1] Zhou, W.; Jin, K., "Efficiency Evaluation of Laser Diode in Different Driving Modes for Wireless Power Transmission", IEEE Transactions on Power Electronics, vol. 30, no. 11, pp. 6237-6244 (2015).
- [2] Sato, F.; Murakami, J.; Suzuki, T.; Matsuki, H.; Kikuchi, S.; Harakawa, K.; Osada, H.; Seki, K., "Contactless energy transmission to mobile loads by CLPS-test driving of an EV with starter batteries", IEEE Transactions on Magnetics, vol. 33, no. 5, pp. 4203-4205 (1997).
- [3] Covic, G. A.; Boys, J. T.; Kissin, M. L. G.; Lu, H. G., "A Three-Phase Inductive Power Transfer System for Roadway-Powered Vehicles", IEEE Transactions on Industrial Electronics, vol. 54, no. 6, pp. 3370-3378 (2007).
- [4] Liu, X.; Hui, S. Y., "Simulation Study and Experimental Verification of a Universal Contactless Battery Charging Platform With Localized Charging Features", IEEE Transactions on Power Electronics, vol. 22, no. 6, pp. 2202-2210 (2007).
- [5] Liu, X.; Hui, S. Y., "Optimal Design of a Hybrid Coil Structure for Planar Contactless Battery Charging Platform", IEEE Transactions on Power Electronics, vol. 23, no. 1, pp. 455-463 (2008).
- [6] Achterberg, J.; Lomonova, E. A.; Boeij, J. d., "Coil Array Structures Compared for Contactless Battery Charging Platform", IEEE Transactions on Magnetics, vol. 44, no. 5, pp. 617-622 (2008).
- [7] Covic, G. A.; Elliott, G.; Stielau,O. H.; Green, R. M.; Boys, J. T., "The design of a contact-less energy transfer system for a people mover system", in International Conference on Power System Technology, pp. 79-84 (2000).
- [8] Sokal, N. O.; Sokal, A. D., "Class E-A new class of high-efficiency tuned single-ended switching power amplifiers", IEEE Journal of Solid-State Circuits, vol. 10, no. 3, pp. 168-176 (1975).
- [9] Aldhaher, S.; Luk, P. C. K.; Whidborne, J. F., "Wireless power transfer using Class E inverter with saturable DC-feed inductor", in IEEE Energy Conversion Congress and Exposition, pp. 1902-1909 (2013).
- [10] Aldhaher, S.; Luk, P. C. K.; Whidborne, J. F., "Tuning Class E Inverters Applied in Inductive Links Using Saturable Reactors", IEEE Transactions on Power Electronics, vol. 29, no. 6, pp. 2969-2978 (2014).
- [11] Mediano, A.; Sokal,N. O., "A Class-E RF power amplifier with a flattop transistor-voltage waveform", IEEE Transactions on Power Electronics, vol. 28, no. 11, pp. 5215-5221 (2013).
- [12] Kaczmarczyk, Z., "High-efficiency Class E, EF2, and E/F3 inverters", IEEE Transactions on Industrial Electronics, vol. 53, no. 5, pp. 1584-1593 (2006).
- [13] Kee, S. D.; Aoki, I.; Hajimiri, A.; Rutledge, D., "The class-E/F family of ZVS switching amplifiers", IEEE Transactions on Microwave Theory and Techniques, vol. 51, no. 6, pp. 1677-1690 (2003).
- [14] Grebennikov, A., "High-Efficiency Class E/F Lumped and Transmission-Line Power Amplifiers", IEEE Transactions on Microwave Theory and Techniques, vol. 59, no. 6, pp. 1579-1588 (2011).
- [15] Hayati, M.; Sheikhi, A.; Grebennikov, A., "Effect of nonlinearity of parasitic capacitance on analysis and design of Class E/F3 power amplifier", IEEE Transactions on Power Electronics, vol. 30, no. 8, pp. 4404-4411 (2015).
- [16] Rivas, J. M.; Han, Y.; Leitermann, O.; Sagneri, A. D.; Perreault, D. J., "A High-Frequency Resonant Inverter Topology With Low-Voltage Stress", IEEE Transactions on Power Electronics, vol. 23, no. 4, pp. 1759-1771 (2008).
- [17] Green, A. W.; Boys, J. T., "10 kHz inductively coupled power transfer-concept and control", in Fifth International Conference on Power Electronics and Variable-Speed Drives, pp. 694-699 (1994).
- [18] Fotopoulos, K.; Flynn, B. W., "Wireless Power Transfer in Loosely Coupled Links: Coil Misalignment Model", IEEE Transactions on Magnetics, vol. 47, no. 2, pp. 416-430 (2011).
- [19] Ho, S. L.; Wang, J.; Fu, W. N.; Sun, M., "A Comparative Study Between Novel Witricity and Traditional Inductive Magnetic Coupling in Wireless Charging", IEEE Transactions on Magnetics, vol. 47, no. 5, pp. 1522-1525 (2011).
- [20] Mizuno, T.; Yachi, S.; Kamiya, A.; Yamamoto, D., "Improvement in Efficiency of Wireless Power Transfer of Magnetic Resonant Coupling Using Magnetoplated Wire", IEEE Transactions on Magnetics, vol. 47, no. 10, pp. 4445-4448 (2011).
- [21] Zhang, F.; Hackworth, S. A.; Fu, W.; Li, C.; Mao, Z.; Sun, M., "Relay Effect of Wireless Power Transfer Using Strongly Coupled Magnetic Resonances", IEEE Transactions on Magnetics, vol. 47, no. 5, pp. 1478-1481 (2011).
- [22] Madsen, M.; Knott, A.; Andersen, M. A. E., "Low Power Very High Frequency Switch-Mode Power Supply With 50 V Input and 5 V Output", IEEE Transactions on Power Electronics, vol. 29, no. 12, pp. 6569-6580 (2014).
- [23] Aldhaher, S.; Yates, D. C.; Mitcheson, P. D., "Modeling and Analysis of Class EF and Class E/F Inverters with Series-Tuned Resonant Networks", IEEE Transactions on Power Electronics, vol. 31, no. 5, pp. 3415-3430 (2016).